Packaging of viral microRNAs in gammaherpesvirus 68

Jessica Lutz

Molecular, Cellular, & Developmental Biology Departmental Honors Thesis
University of Colorado at Boulder

April 4, 2013

Thesis Advisor
Jennifer Martin | Honors Council Representative | MCDBiology

Off-Campus Thesis Advisor
Linda van Dyk | Associate Professor | Microbiology
University of Colorado School of Medicine

Committee Members
Nancy Guild | Professor | MCDBiology
Jennifer Kugel | Research Associate Professor | Chemistry & Biochemistry

Abstract

MicroRNAs are a characteristic of many herpesvirus genomes. These short, non-coding RNAs are capable of post-transcriptional regulation of target mRNAs. Recently, packaged miRNAs have been observed in purified virions of EBV and KSHV, gammaherpesviruses pathogenic in humans. Gammaherpesvirus 68 serves as a small-animal model of gammaherpesvirus pathogenesis. It encodes eight RNA pol III transcripts known as TMERs, which include viral tRNA-like genes adjacent to one or two miRNA genes. Here, we focused on the miRNAs of TMERs 1 and 5. We detected viral miRNAs and their precursors in purified virions of wild-type gammaherpesvirus 68, as well as two mutant viruses that do not produce TMERs. This suggests viral miRNA packaging is a preferred, organized process in virion maturation. We have also established that these miRNAs are biologically active upon infection.

Table of Contents

List of Figures

Introduction

MicroRNAs

MicroRNAs (miRNAs) are small noncoding RNAs of 20-25 nucleotides that regulate post-transcriptional gene expression. MiRNAs were first identified in *Caenorhabditis elegans* as small temporal RNAs that served in developmental regulation. It soon became apparent that these stRNAs were members of a large miRNA family, with a variety of expression patterns and regulatory targets. Since then, thousands of miRNAs have been identified, including many mammalian and plant miRNAs (He and Hammond, 2004).

MicroRNA biogenesis and function

The canonical miRNA biogenesis pathway begins in the nucleus with the transcription of a primary miRNA (pri-miRNA) transcript by RNA polymerase II (Lee et al., 2004) (Figure 1). Transcription by RNA polymerase III has also been observed (Borchert et al., 2006). Local folding of the pri-miRNA transcript results in a stem-loop of 60-70 nucleotides, with the miRNA coding sequence in the stem. Drosha, an RNase-III enzyme, recognizes the stem-loop structure and cleaves it out of the primary transcript to create precursor-miRNA (pre-miRNA). Exportin 5 then exports the pre-miRNA from the nucleus to the cytoplasm where it is recognized by Dicer, another RNase-III enzyme. Dicer produces functional mature miRNAs with 5' monophosphate and 3' hydroxyl ends in a miRNA duplex (Diebel, 2009). The miRNA duplex stem with the maturely processed miRNA is incorporated into the RNA-induced silencing complex (RISC), composed mainly of argonaute proteins 1-4, and can be directed to target mRNAs (He and Hammond, 2004; Lee et al., 2004).

Binding between the miRISC and its target mRNA occurs through interactions between the seed sequence of the miRNA, found at the 5' end, and the seed match of the target mRNA, found in the 3' UTR. In most cases, the miRISC only requires perfect base pairing between the seed sequence and the seed match to inhibit translation or degrade the mRNA. Seed sequences are short, only six to eight

nucleotides in length, and miRNAs are therefore believed to have multiple mRNA targets (He and Hammond, 2004). In less common cases, a miRNA associates with argonaute protein 2 (Ago 2) and the complex cleaves target sequences of perfect complementarity to the entire miRNA (Diebel et al., 2010) (Figure 1).

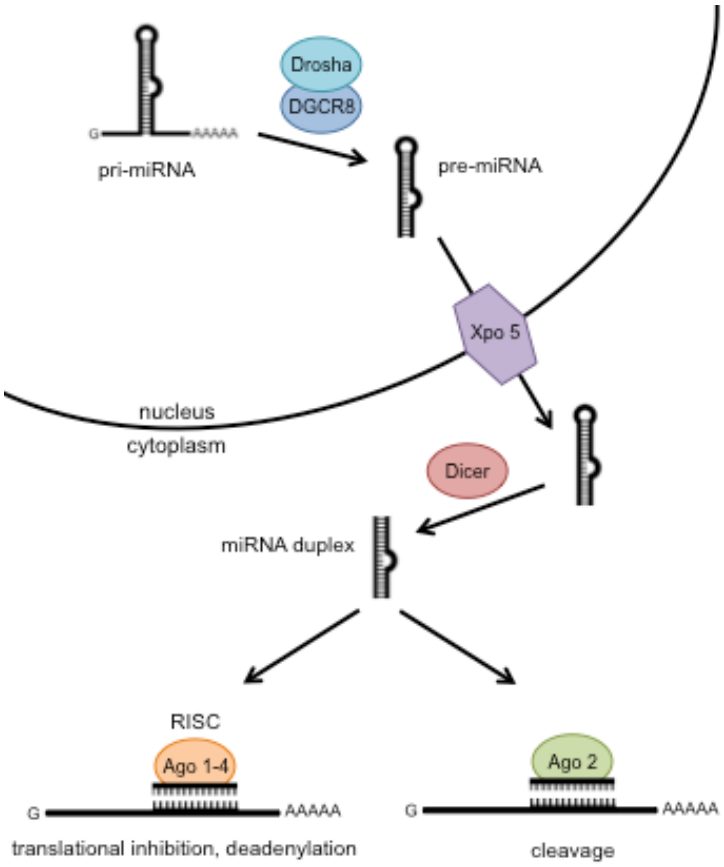

Figure 1. MiRNA biogenesis and function. MiRNA biogenesis begins in the nucleus with transcription by RNA pol II or III to create pri-miRNA. Drosha cleavage produces a pre-miRNA transcript that is exported into the cytoplasm by Exportin 5 (Xpo 5). Dicer cleavage results in maturely processed miRNA in a miRNA duplex, and the miRNA is quickly incorporated into RISCs. MiRISCs inhibit translation and degrade mRNA targets, determined by the seed sequence of the miRNA. In some cases, miRNA associated with Ago 2 will cleave mRNA sequences of perfect complementarity.

MiRNAs are of particular interest to virologists, specifically those studying double-stranded DNA viruses. Since the initial discovery of miRNAs of viral origin in 2004, over 200 viral miRNAs have been identified. These miRNAs have the ability to assist in various viral mechanisms, as well as disrupt cellular processes. Viral miRNAs have been observed in multiple nuclear DNA viruses, including polyomaviruses, but the bulk of miRNAs of viral origin to date have been found in herpesviruses (Plaisance-Bonstaff and Renne, 2011).

Herpesviruses

Herpesviruses, members of the *Herpesviridae* family, are found abundantly in nature and are able to establish lifelong host infections. Over 200 herpesviruses have been identified, and five percent readily infect humans. All herpesviruses contain large, double-stranded DNA genomes and appear to share four biological properties: a large quantity of genes involving nucleic acid metabolism, viral DNA synthesis and capsid assembly in the nucleus, destruction of the host cell with the production of new virus, and the ability to remain latent within their hosts (Roizman and Pellet, 2006). Latent infections are associated with the most dangerous pathologies of herpesviruses, including malignant transformations of infected cells (Roizman and Pellet, 2006).

Structure

Herpesvirions typically consist of four structural elements (Figure 2). The core contains a linear double-stranded DNA genome 125 to 290 kbp in length (Davison et al., 2009). The capsid, surrounding the core, is composed of 162 pentameric capsomeres totaling 100 nm in diameter. A protein-rich material surrounding the capsid is known as the tegument (Roizman and Pellet, 2006). The tegument contains viral proteins, host proteins, and RNAs. Although the tegument is not fully understood, many tegument proteins are known to assist the virus immediately upon infection with roles involving entry, gene regulation, and particle assembly (Mettenleiter et al., 2009; Bortz et al., 2003). The envelope surrounds the tegument, containing host lipids and viral glycoproteins (Roizman and Pellet, 2006).

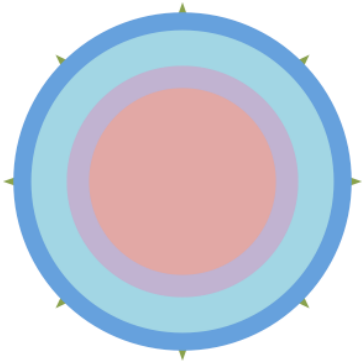

Figure 2. Herpesvirion Structure. An illustration of the four structural elements of the herpesvirion. The core, shown in pink, contains the double-stranded DNA genome. The capsid is shown in purple, surrounded by the tegument, shown in light blue. The tegument is known to contain viral proteins, host proteins, and RNAs. The envelope is shown in dark blue, with glycoproteins in green.

Replication

All herpesviruses have the ability to replicate through lytic or latent infection. Lytic infection results in the destruction of the host cell and production of new infectious virus. It begins with the attachment of the virus to the host cell and release of the nucleocapsid into the cytoplasm. The nucleocapsid travels to the nucleus, where the viral genome circularizes. Genes are transcribed in order, from immediate early genes, to early genes, to late genes. Immediate early genes require no viral protein synthesis to be expressed. Early genes do require viral protein synthesis, and are expressed about 6 hours after the onset of infection. Late genes require the onset of viral DNA replication. Following viral DNA replication, viral DNA is surrounded by newly formed capsids and moves to the cytoplasm. The nucleocapsids are then surrounded by tegument, enveloped, and released from the destroyed host cell (Peng et al., 2010; Roizman and Knipe, 2001) (Figure 3).

Latent infection is established after the circularization of the viral genome. It can occur with or without limited viral gene expression. Herpesviruses are able to establish latent infection in specific host cell-types, and maintenance of latency is cell-type specific. Limited viral gene expression most likely assists with maintenance of latency, including subversion of the host's immune response. Additionally, herpesviruses known to produce miRNAs have been shown to continuously produce them during latency (Diebel, 2009; Pfeffer et al., 2005). Reactivation occurs when the lytic infection is triggered, but events associated with switches between lytic and latent infection are not well understood (Figure 3).

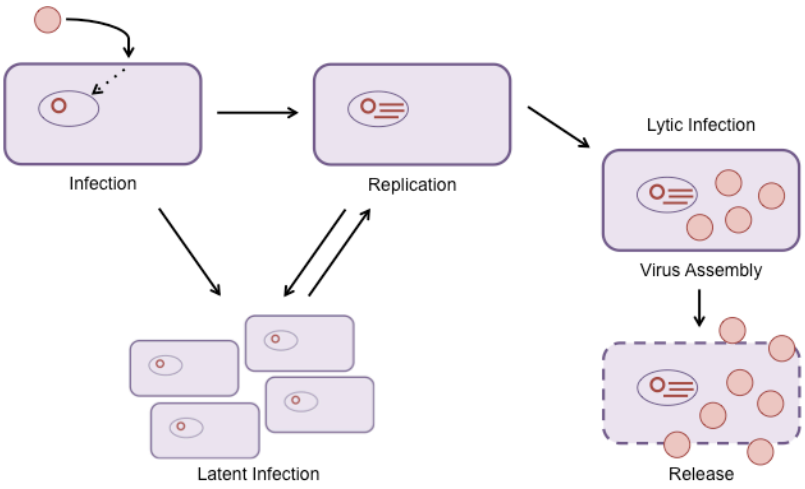

Figure 3. Herpesvirus infection. Herpesviruses are able to establish both lytic and latent infection. Infection begins when the virus attaches to the host cell and the nucleocapsid travels to the nucleus. The viral genome immediately circularizes. Latent infection can occur before or after limited genome expression. Lytic infection results in cell lysis, and involves the expression of the viral genome, virus assembly, and release of infectious virus.

Gammaherpesviruses

Herpesviruses are classified into the three subfamilies *Alphaherpesvirinae*, *Betaherpesvirinae*, and *Gammaherpesvirinae* based on biological properties and DNA sequence homology (Roizman and Pellet, 2006). Gammaherpesviruses are linked to autoimmune diseases, lymphoproliferative diseases, and tumor formation (Virgin and Speck, 1999). *In vitro*, gammaherpesviruses replicate in lymphoblastoid cells, and some are able to establish lytic infection in epithelial and fibroblastoid cells. *In vivo*, gammaherpesviruses are limited to the family of the natural host.

Gammaherpesviruses infect a wide variety of hosts, but only two, EBV and KSHV, are known to be human pathogens (Roizman and Pellet, 2006). Epstein-Barr Virus (EBV) is believed to infect over 90% of the world's population. Most often, EBV infection occurs at a young age and is asymptomatic. Infections occurring after adolescence can result in mononucleosis, a lymphoproliferative disease involving memory B cells (Thorley-Lawson, 2001). EBV infections have been related to Burkitt's lymphoma, Hodgkin's disease, immunoblastic lymphomas, and nasopharyngeal carcinoma (Diebel, 2009). Kaposi's sarcoma-associated herpesvirus (KSHV) is linked to at least four human cancers, including Kaposi sarcoma, Castleman's disease, and two B-cell lymphomas (Thorley-Lawson, 2001).

In 2004, the Tuschl lab at The Rockefeller University made the first observation of viral miRNA expression in EBV (Pfeffer et al., 2004). Since then, miRNAs have been identified in other gammaherpesviruses, including KSHV.

Gammaherpesvirus 68 (γHV68)

EBV and KSHV cannot be studied *in vivo* in a non-human host due to the narrow host range of herpesviruses. Gammaherpesvirus 68 (γHV68) serves as a small animal model for gammaherpesvirus pathogenesis, and readily undergoes lytic infection *in vitro*, allowing researchers to produce large amounts of virus (Diebel, 2009). γHV68 was originally isolated from a bank-vole in Slovakia and naturally infects wild murid rodents. Like EBV and KSHV, miRNAs have been identified in γHV68.

Gammaherpesvirus 68 miRNAs

The left end of the γHV68 genome contains two ORFs, (M1 and M2), and eight RNA pol III transcripts, known as TMERs (Diebel et al., 2010) (Figure 4). M1 and M2 are considered non-essential genes, and encode a secreted protein that activates Vβ4+ CD8+ T cells and an adaptor protein involved in B cell differentiation (Barton et al., 2011). The miRNAs of γHV68 are all contained within the TMERs, and are named miR-M1-1 through 15 (Figure 4).

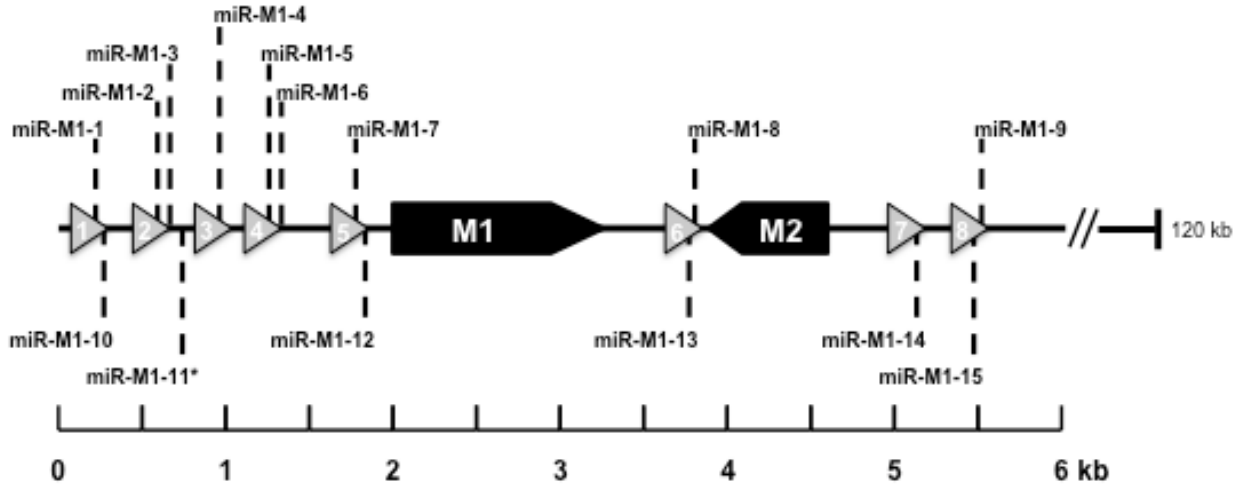

Figure 4. The left end of the γHV68 genome. The left 6 kb of the γHV68 genome. Gray numbered arrows represent TMERs 1 through 8. MiRNAs (miR-M1-1 through 15) are labeled with dashed lines. The M1 and M2 ORFs are shown in black.

TMERs are divided into three sections based on their predicted secondary structures: a tRNA-like region, stem-loop 1, and stem-loop 2 (Figure 5). RNA pol III promoter elements are located in the tRNA-like region. The tRNA-like region produces vtRNA transcripts, which are processed similarly to cellular tRNAs, including the addition of 3' CCA nucleotides. There is no evidence of aminoacylation, however, and the function of vtRNAs is unknown (Bowden et al., 1997; Diebel, 2009).

γHV68 miRNAs are all contained within the stem-loop 1 and stem-loop 2 regions of the TMERs (Figure 5). An alternate stop exists between stem-loops 1 and 2, and miRNAs located in stem-loop 2 are found in lower abundance during viral infection (Reese, 2010; Zhu 2010).

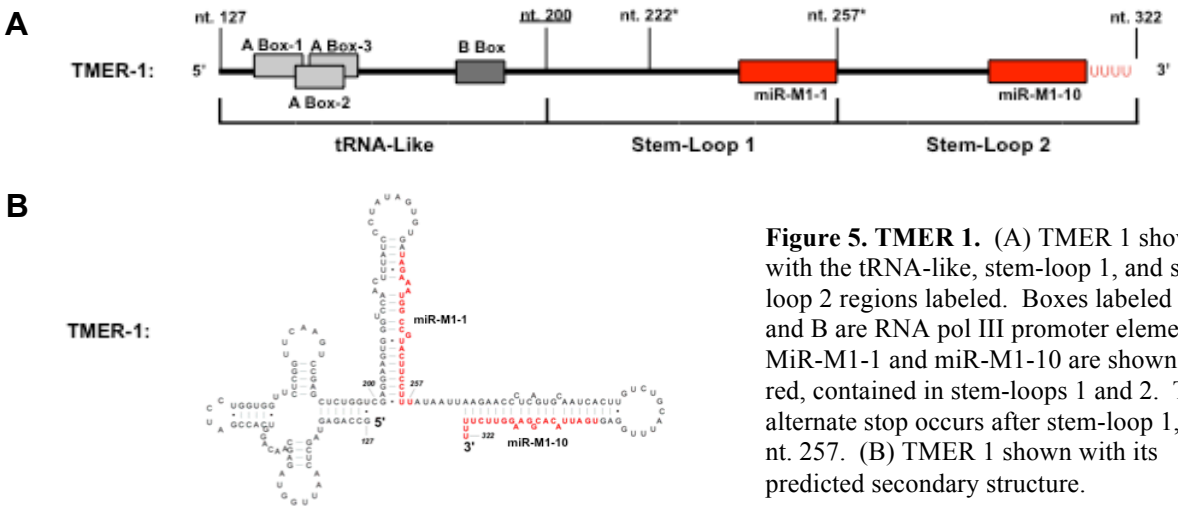

Figure 5. TMER 1. (A) TMER 1 shown with the tRNA-like, stem-loop 1, and stem-loop 2 regions labeled. Boxes labeled A and B are RNA pol III promoter elements. MiR-M1-1 and miR-M1-10 are shown in red, contained in stem-loops 1 and 2. The alternate stop occurs after stem-loop 1, at nt. 257. (B) TMER 1 shown with its predicted secondary structure.

Processing of miRNAs within TMER transcripts is similar to canonical miRNA processing, with a few known exceptions. As mentioned, TMERs are transcribed by RNA pol III. RNase Z, an enzyme responsible for tRNA maturation at the 3' end, cleaves off the tRNA-like portion of the transcript. Drosha and Dicer cleavages still occur (Diebel et al., 2010) (Figure 6).

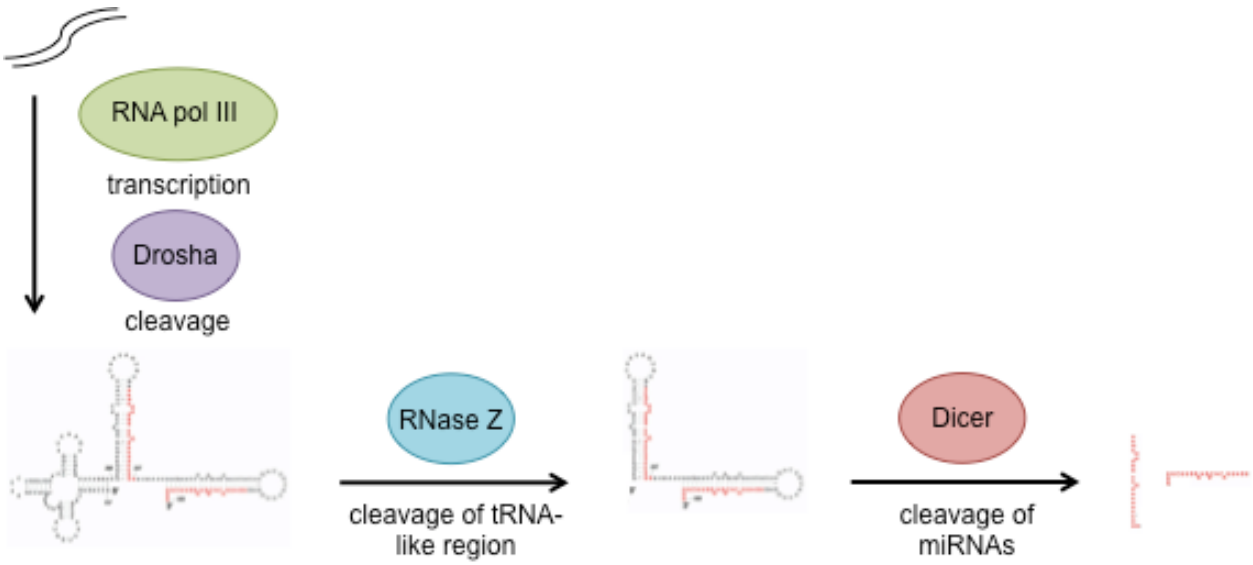

Figure 6. TMER processing. TMERs are transcribed by RNA pol III, and RNase Z cleaves the tRNA-like region from the stem-loops. Canonical processing events, (including Drosha cleavage and Exportin 5 transport), still occur. Dicer produces mature miRNAs.

Mutant Virus Models

The van Dyk lab possesses two mutant virus models used in this project: TKO.γHV68 and γHV68Δ9473. The TKO.γHV68 virus lacks the ability to produce TMER transcripts due to deletions of the RNA pol III promoters associated with all eight of the γHV68 TMER genes (Diebel et al., in press). This virus therefore also lacks the ability to produce the γHV68 miRNAs. γHV68Δ9473 lacks the entire left end of the γHV68 genome, and therefore cannot produce any of the TMERs or M1 through M4 (Clambey et al., 2002). Interestingly, TKO.γHV68 shows diminished infectivity in 3T12 cells when compared to wild type γHV68, while γHV68Δ9473 does not (Clambey et al., 2002; Diebel et al., in press). The lab is currently transitioning from using γHV68Δ9473 to TKO.γHV68.

Viral miRNA packaging

The tegument of herpesvirions is known to contain viral and cellular proteins that assist with viral infection (Penkert and Kalejta, 2011). If packaged, mature viral miRNAs would also have the potential to act immediately upon infection. Over the past two years, packaged maturely processed viral miRNAs have been observed in purified virions of gammaherpesviruses EBV and KSHV (Jochum et al., 2011; Lin et al., 2012). Additionally, packaged viral miRNAs have been observed in purified virions of the Herpes B alphavirus, and packaged cellular miRNAs have been observed in HIV-1 virions (Amen and Griffiths, 2011; Schopman et al., 2012).

In 2009, the Dutia lab at the University of Edinburgh observed γHV68 vtRNAs packaged in purified γHV68 virions (Cliffe et al., 2009). Packaging of TMER miRNAs, however, has not previously been examined.

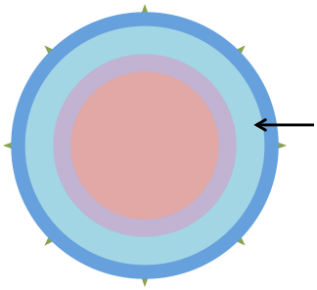

Figure 7. Packaging in the tegument. Packaged viral miRNAs are most likely housed in the tegument, shown with the black arrow, which also contains viral and cellular proteins.

Project objectives

This project stems from the recent observations of miRNA and vtRNA packaging in gammherpesviruses. I have two main goals: to determine whether TMER miRNAs or their precursors are packaged in γHV68 virions, and whether these packaged miRNAs are biologically functional. This also involves observations of packaging in trans by the TKO.γHV68 and γHV68Δ9473 mutant viruses. I focus on the miRNAs of TMERs 1 and 5, specifically miR-M1-1, miR-M1-10, miR-M1-7-3p, and miR-M1-12. My research establishes that viral miRNAs and their precursors are packaged by γHV68, as well as in trans by the mutant viruses, and are biologically active upon infection.

Results

Unprocessed and processed forms of TMERs 1 and 5 are present in purified virions. To determine the presence of miRNAs in the γHV68 virion, we performed RLM-RT-PCR on RNA isolated from purified virions. γHV68 virions were purified from infected 3T12 cells as previously described (Cliffe et al., 2009) (Figure 8A). RLM-RT-PCR allows for amplification of mature miRNAs because it utilizes T4 RNA ligase, an enzyme that ligates single stranded nucleic acids as long as one strand contains a 5' monophosphate and the other a 3' hydroxyl end. Mature miRNAs are sufficient substrates for RLM-RT-PCR because they are products of Dicer cleavage, which leaves a 5' monophosphate and 3' hydroxyl end. Two synthetic RNA linker oligos were previously designed: one with hydroxyl groups at both the 5' and 3' ends for ligation to miRNAs from the 3' stem of a pre-miRNA stem loop, and one with a 5' monophosphate for ligation to miRNAs found on the 5' stem of a pre-miRNA stem loop (Diebel et al., 2010). All miRNAs studied in this project arise from the 5' stem of a pre-miRNA stem loop, except for

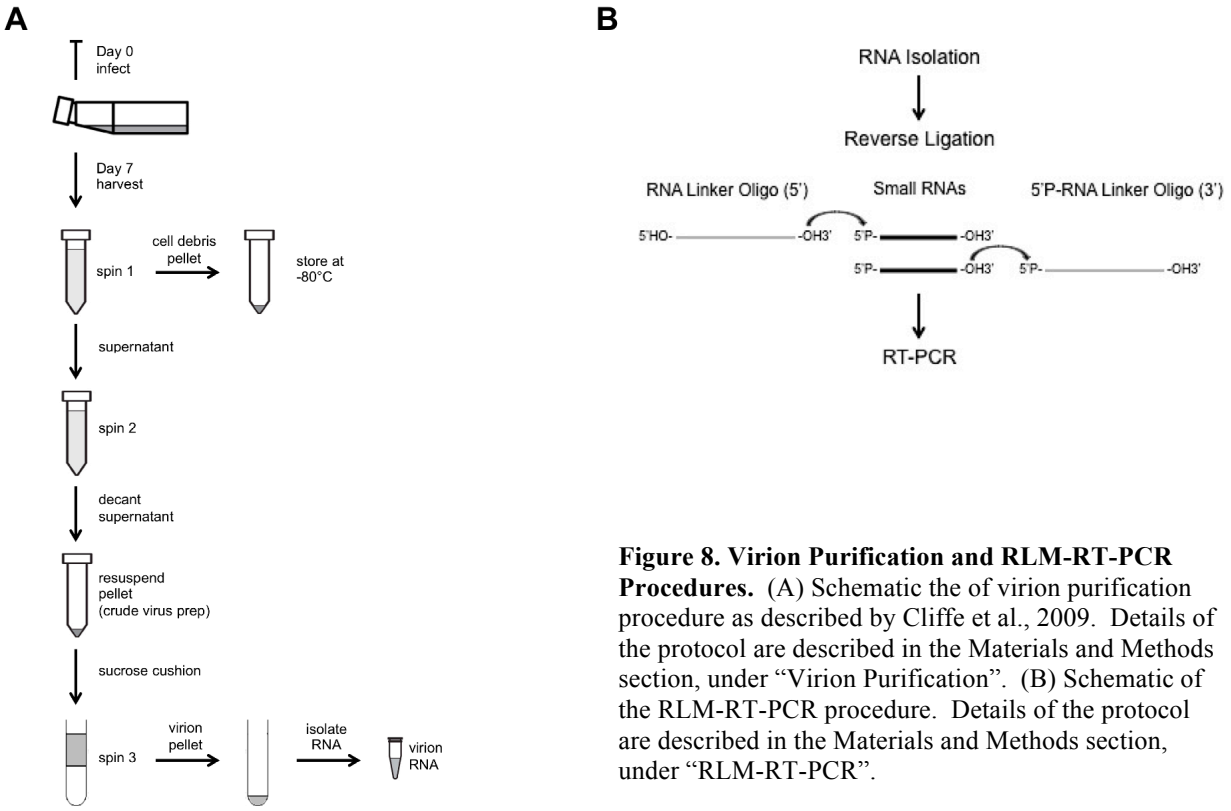

Figure 8. Virion Purification and RLM-RT-PCR Procedures. (A) Schematic the of virion purification procedure as described by Cliffe et al., 2009. Details of the protocol are described in the Materials and Methods section, under "Virion Purification". (B) Schematic of the RLM-RT-PCR procedure. Details of the protocol are described in the Materials and Methods section, under "RLM-RT-PCR".

the mouse miRNA mmu-miR-21, used as a cellular control. After ligation of the mature miRNA to the RNA linker oligo, RT-PCR analysis was conducted with the miRNA sequence as one primer binding site and the RNA linker oligo as the other primer binding site (Figure 8B).

RLM-RT-PCR was first performed on purified γHV68 virions following 3T12 infection using primer sets for mature miR-M1-1 and miR-M1-7-3p (Figure 9A). Amplicon product sizes of 38 base pairs were expected and observed, indicating the presence of maturely processed miR-M1-1 and miR-M1-7-3p viral miRNAs in the γHV68 virions. MiR-M1-1 was further analyzed using RLM-RT-PCR with primers to detect both the mature miRNA and the pre-miRNA stem loop 1 viral RNAs (Figure 9B). Product sizes of 38 and 70 base pairs were expected, respectively. The expected product size was observed again for mature miR-M1-1, but the pre-miRNA stem loop primer produced a doublet above its expected size.

Both the mature miR-M1-1 primer product and the doublet product of the pre-miRNA stem loop primer were cloned and sequenced (Figure 9E). Sequence analysis revealed the mature miR-M1-1 primer identified perfect mature miR-M1-1 in ten out of twelve sequences, with two read-throughs (Figure 9E, C). Analysis of the doublet product of the pre-miRNA stem loop primer never yielded an exact match for the pre-miRNA stem loop, with six of twelve sequences being of viral origin but of longer length than the pre-miRNA stem loop (Figure 9E, D). This is potentially indicative of the presence of full-length TMER 1 in various stages of degradation, although to create products with RLM-RT-PCR, this degradation must create 5' monophosphates. Analysis also revealed that the primer was less specifically binding than intended, showing non-specific mmu mitochondrial 16S rRNA in five out of twelve sequences, as well as non-specific mmu chromosome 17 mRNA in one sequence (Figure 9E).

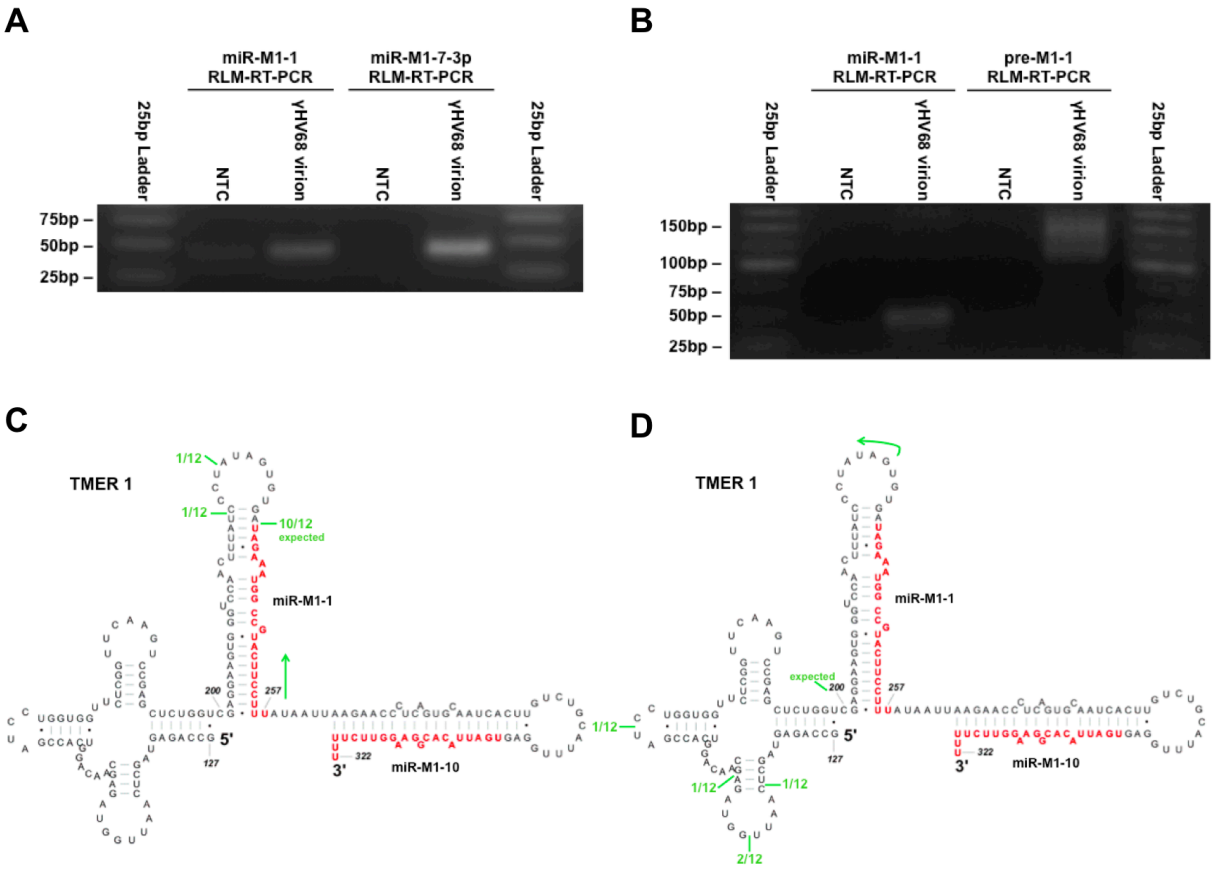

E

miR-M1-1:	UUUCCUUCAUGCCGGUAAAGAU	# clones
miR-M1-1 RLM-RT-PCR	UUUCCUUCAUGCCGGUAAAGAU	10
	UUUCCUUCAUGCCGGUAAAGAUAGUGUGAUA	1
	UUUCCUUCAUGCCGGUAAAGAUAGUGUGAUAUCCC	1

pre-M1-1 expected product:	GAUAUCCCUAUUUCAACCUGGGUGAAGGAG	# clones
pre-M1-1 RLM-RT-PCR	GAUAUCCCUAUUUCAACCUGGGUGAAGGAGCUGGUCUCGAGCCU GAACUUGGCUCUUGGUGGUCC	1
	GAUAUCCCUAUUUCAACCUGGGUGAAGGAGCUGGUCUCGAGCCU GAACUUGGCUCUUGGUGGUCCUAGCCACUGGACAACG	1
	GAUAUCCCUAUUUCAACCUGGGUGAAGGAGCUGGUCUCGAGCCU GAACUUGGCUCUUGGUGGUCCUAGCCACUGGACAACGAGAUGG	2
	GAUAUCCCUAUUUCAACCUGGGUGAAGGAGCUGGUCUCGAGCCU GAACUUGGCUCUUGGUGGUCCUAGCCACUGGACAACGAGAUGGUUAAC	1
	GAUAUCCCUAUUUCAACCUGGGUGAAGGAGCUGGUCUCGAGCCU GAACUUGGCUCUUGGUGGUCCUAGCCACUGGACAACGAGAUGGUUAAC UCGAUGAGACCGUGGUCGUGUU	1
	non-specific mmu mitochondrial 16S rRNA	5
	non-specific mmu chromosome 17 mRNA	1

Figure 9. Unprocessed and processed forms of TMERs 1 and 5 are present in purified virions. (A) RLM-RT-PCR of mature miR-M1-1 and miR-M1-7-3p from purified γHV68 virions following 3T12 infection. Products were resolved by gel electrophoresis and visualized by ethidium bromide. (B) RLM-RT-PCR for mature miR-M1-1 and the pre-miR-M1-1 stem loop 1 ("pre-M1-1") from purified γHV68 virions. (C) Illustration of cloned and sequenced products from mature miR-M1-1 RLM-RT-PCR. Green marks represent product locations. (D) Illustration of cloned and sequenced products from pre-miRNA stem loop ("pre-M1-1") RLM-RT-PCR. (E) Results of sequencing reactions. Nucleotides in black represent expected products.

Northern blot analysis for TMER 1 and TMER 5 from purified virions. As described, RLM-RT-PCR cannot detect RNAs without 5' monophosphates, so we used northern blots to identify other potential transcripts of TMERs present in the virion. Previous northern blot analyses of TMER 1 on total RNA collected during γHV68 lytic infection has yielded three bands of 195, 130, and 53 nucleotides in length, predicted to represent the full-length transcript, the tRNA-like region + pre-miRNA stem loop 1, and pre-miRNA stem loop 1, respectively, (miR-M1-1 has not been detectable with this analysis) (Diebel et al., 2010) (Figure 10A).

Our northern blot analysis was again focused on TMERs 1 and 5, to determine the presence and size of different regions packaged in the γHV68 virion. TMER 1 was analyzed using a 5'-biotinylated probe that anneals perfectly to the miR-M1-1 sequence, and TMER 5 was analyzed using a 5'-biotinylated probe that anneals perfectly to the miR-M1-7-3p sequence. TMER 1 analysis was performed on total RNA isolated from purified γHV68 virions following 3T12 cell infection. TMER 5 analysis was performed on total RNA isolated from purified γHV68 virions following 3T12 cell infection, 3T12 cell debris after γHV68 infection, and mock uninfected 3T12 cells. Sizes of detected bands were assigned based on gel migration comparison with size standard markers.

We observed a somewhat novel banding pattern from these analyses of purified virion (Figure 10E). The standard three bands between 50 and 200 nt in length were detected in the γHV68 virions probed for miR-M1-1 and miR-M1-7-3p; however, both also demonstrated doublets involving the top two bands. The γHV68 infection 3T12 cell debris showed the same faint banding pattern, and the mock uninfected 3T12 cells revealed no detectable bands, as expected. Based on assignment of band sizes from comparison with size standard markers, it appears that the top bands of the doublets correspond to the full-length transcript (~200 nt) and the tRNA-like region + pre-miRNA stem loop 1 (~130 nt). The lowest band (~50 nt) corresponds to pre-miRNA stem loop 1. The identities of the lower doublet bands are unknown, and speculated to be a result of TMER processing events or degradation. To be certain of these comparisons, the samples will need to be run next to total RNA collected during γHV68 lytic infection used during previous analyses.

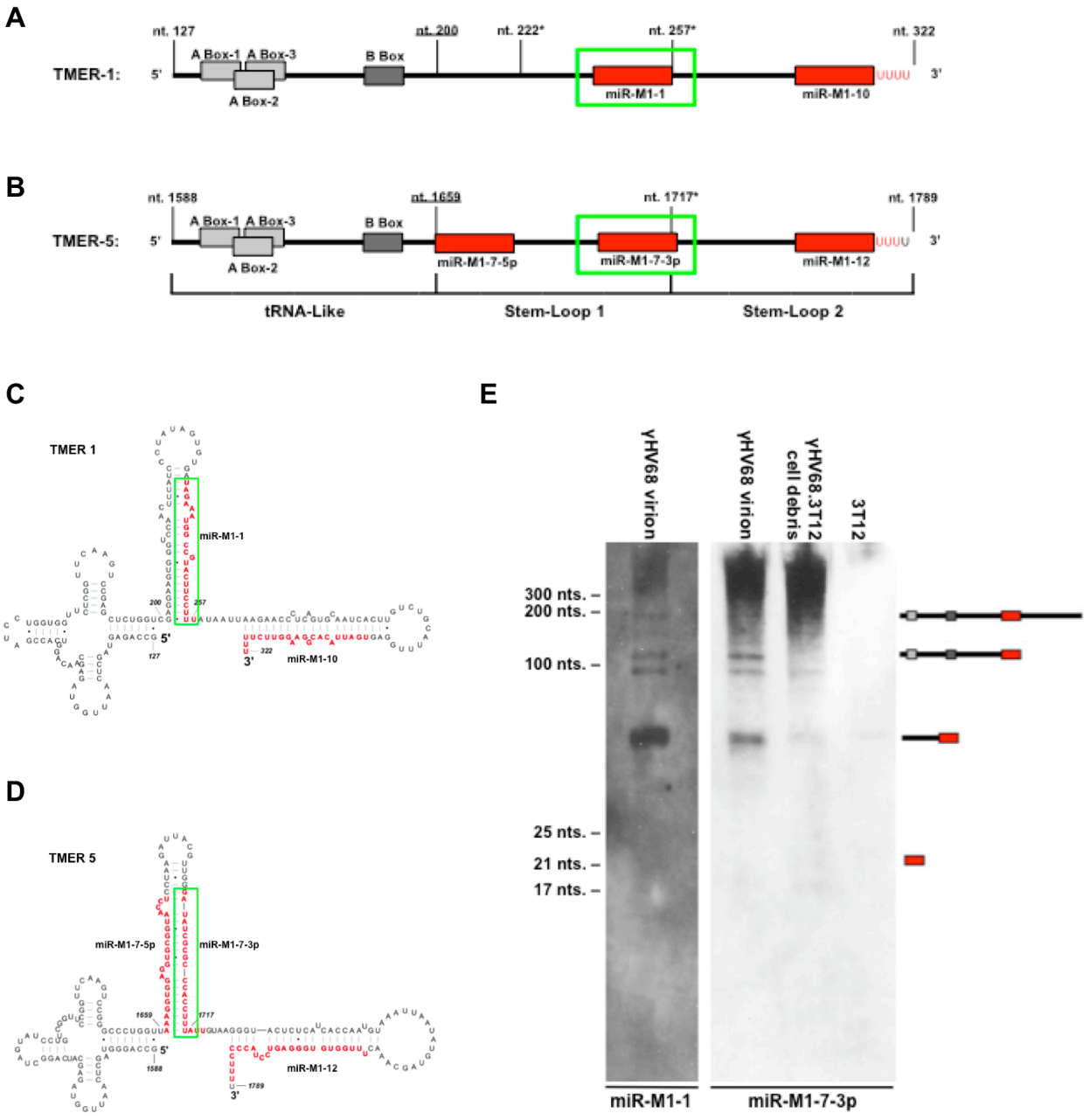

Figure 10. Northern blot analysis for TMER 1 and TMER 5 from purified virions. (A) Illustration of TMER 1, showing the tRNA-like, stem-loop 1, and stem-loop 2 regions. A and B boxes are promoter elements that drive RNA pol III transcription. Starred numbers are alternative stop sequences. (B) Illustration of TMER 5, showing the tRNA-like, stem-loop 1, and stem-loop 2 regions. (C) Illustration of TMER 1 with its predicted secondary structure. MiR-M1-1 is outlined in green. (D) Illustration of TMER 5 with its predicted secondary structure. MiR-M1-7-3p is outlined in green. (E) Northern blot analysis of TMER 1 on RNA isolated from purified γHV68 virions following 3T12 cell infection, and TMER 5 on RNA isolated from purified γHV68 virions following 3T12 cell infection, 3T12 cell debris after γHV68 infection, and mock uninfected 3T12 cells. Potential products are shown to the right of the blot. (Potential products from top to bottom: full-length TMER, tRNA-like region + stem loop 1, stem loop 1, miRNA.)

MiR-M1-1 and miR-M1-7-3p are packaged in trans by the TKO.γHV68 mutant virus. We used the recently developed TKO.γHV68 virus and LE stably transfected cell line to examine the ability of TKO.γHV68 to package viral miRNAs in trans. The TKO.γHV68 virus lacks the ability to produce the TMER transcripts due to deletions of the RNA pol III promoters associated with all eight of the γHV68 TMER genes. This virus therefore also lacks the ability to produce the γHV68 miRNAs, including miR-M1-1 and miR-M1-7-3p (Diebel et al., in press). The LE stably transfected cell line is stably transfected with a plasmid containing the complete left end of the γHV68 genome, and therefore produces TMERs and their miRNAs.

In order to assess the ability of TKO.γHV68 to package miRNAs in trans, TKO.γHV68 virions were purified after infection of the LE stably transfected cell line. Total RNA isolated from purified virions was analyzed by RLM-RT-PCR, using primers for maturely processed miR-M1-1 and miR-M1-7-3p (Figure 11). These samples were run along with total RNA isolated from purified γHV68 virions following infection of 3T12 cells, 3T12 cell debris after γHV68 infection, uninfected LE stably transfected cells, 3T12 cell debris after TKO.γHV68 infection, and mock uninfected 3T12 cells. The mmu miRNA 21 served as a cellular control.

As expected, the 3T12 cell debris after TKO.γHV68 infection and mock uninfected 3T12 cells yielded no PCR product from either miRNA primer set, as neither sample involved the production of TMERs. Both miR-M1-1 and miR-M1-7-3p primer sets yielded the expected products of 38 bp from purified TKO.γHV68 virions following LE cell infection and from purified γHV68 virions following infection of 3T12 cells, as well as 3T12 cell debris after γHV68 infection and the LE stably transfected cells. The presence of miR-M1-1 and miR-M1-7-3p was previously observed in purified γHV68 virions following infection of 3T12 cells, and was therefore expected in 3T12 cell debris after γHV68 infection (Figure 10). The expected product from LE stably transfected cells confirmed their production of miR-M1-1 and miR-M1-7-3p, although their products have consistently appeared slightly larger than the miRNA products produced in the presence of virus. These products must be sequenced to confirm the possibility of processing events associated with viral infection. Most notably, although TKO.γHV68 does

not have the ability to produce miR-M1-1 or miR-M1-7-3p on its own, it does have the ability to package these miRNAs in trans. This indicates that miRNAs are purposefully packaged into γHV68 virions.

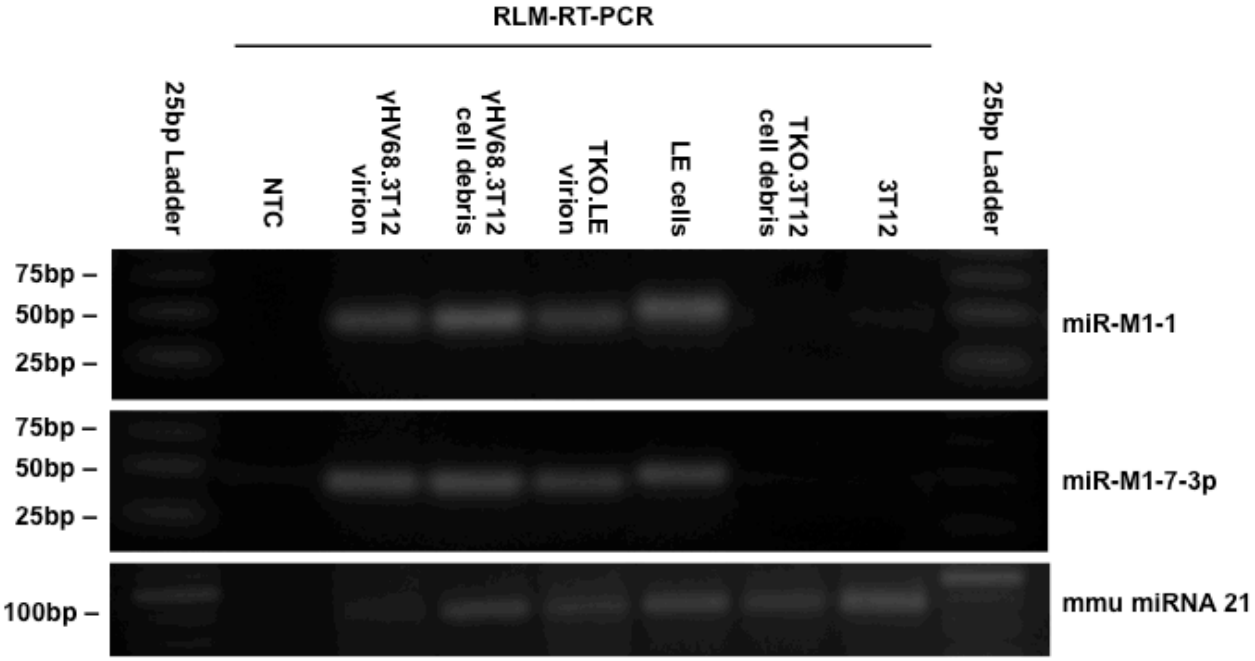

Figure 11. MiR-M1-1 and miR-M1-7-3p are packaged in trans by TKO.γHV68. RLM-RT-PCR of mature miR-M1-1 and miR-M1-7-3p from purified γHV68 virions following 3T12 infection, 3T12 cell debris after γHV68 infection, purified TKO.γHV68 virions following LE cell infection, LE stably transfected cells, 3T12 cell debris after TKO.γHV68 infection, and mock uninfected 3T12 cells. mmu miRNA 21 serves as a cell control. Products were resolved by gel electrophoresis and visualized by ethidium bromide.

RLM-RT-PCR analysis for miR-M1-10 and miR-M1-12 reveals miRNA packaging in γHV68 is potentially selective. To further investigate packaging of miRNAs in the γHV68 virion, the RLM-RT-PCR from the previous experiment was extended to include primer sets for miR-M1-10 and miR-M1-12 (Figure 12A). miR-M1-10 and miR-M1-12 are miRNAs that occur in the second stem-loops of TMERs 1 and 5, respectively (Figure 12B, C). Both miRNAs follow the alternate stops in the TMERs, and appear to be produced at a lower frequency than miR-M1-1 and miR-M1-7-3p (Reese, 2010; Zhu, 2010). Again, total RNA isolated from purified γHV68 virions following infection of 3T12 cells, 3T12 cell debris after γHV68 infection, purified TKO.γHV68 virions following infection of the LE containing cells, uninfected LE stably transfected cells, 3T12 cell debris after TKO.γHV68 infection, and mock

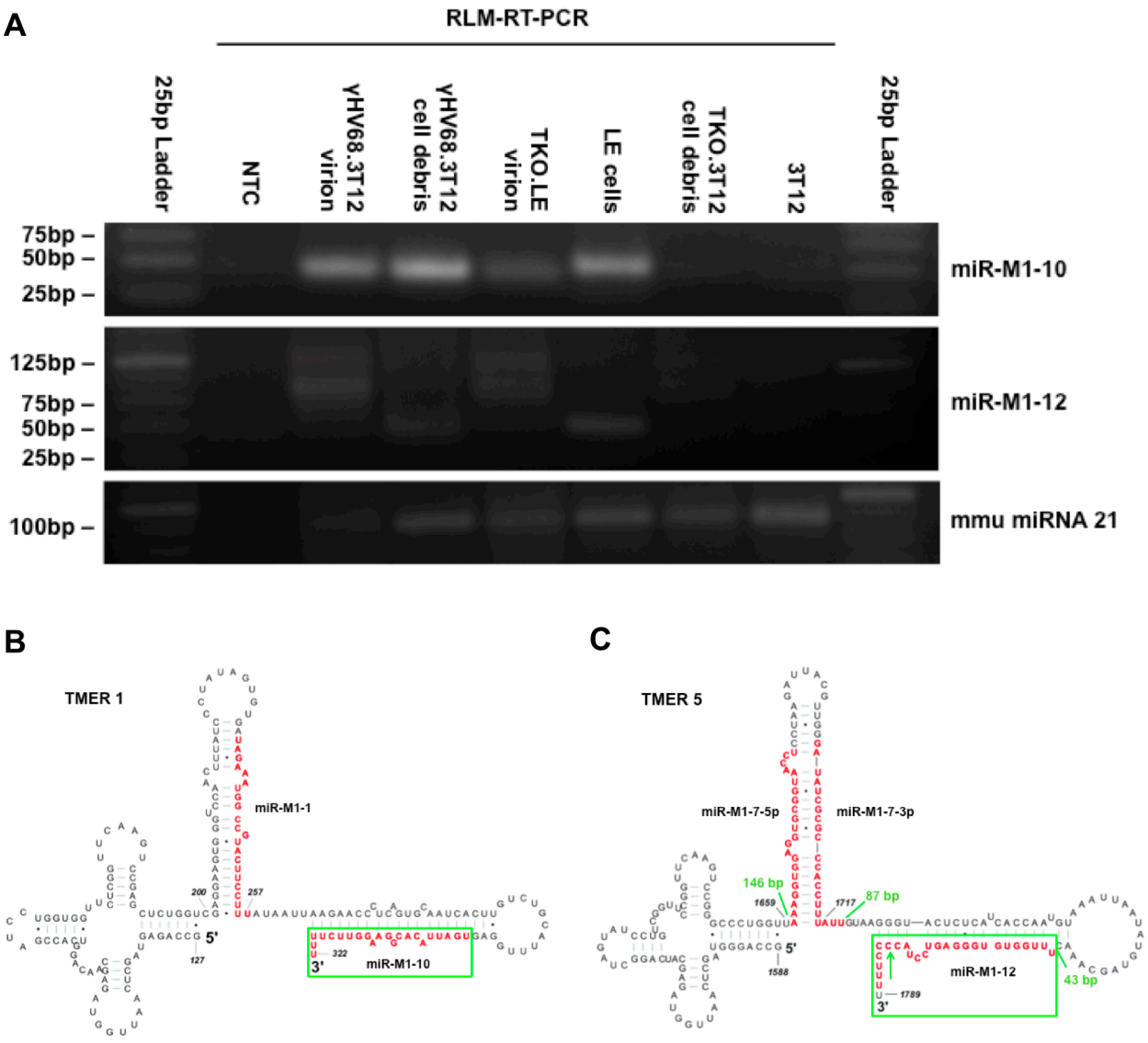

Figure 12. RLM-RT-PCR analysis for miR-M1-10 and miR-M1-12 reveals miRNA packaging in γHV68 is potentially selective. (A) RLM-RT-PCR of mature miR-M1-10 and miR-M1-12 from purified γHV68 virions following 3T12 infection, 3T12 cell debris after γHV68 infection, purified TKO.γHV68 virions following LE cell infection, LE stably transfected cells, 3T12 cell debris after TKO.γHV68 infection, and mock uninfected 3T12 cells. Mmu miRNA 21 serves as a cell control. Products were resolved by gel electrophoresis and visualized by ethidium bromide. (B) Illustration of TMER 1 with its predicted secondary structure. MiR-M1-10 is outlined in green; product size is 41 bp. (C) Illustration of TMER 5 with its predicted secondary structure. MiR-M1-12 is outlined in green, and green labels represent potential products of RLM-RT-PCR with their ligated product size.

uninfected 3T12 cells were analyzed. The mmu miRNA 21 served as a cellular control.

RLM-RT-PCR analysis of miR-M1-10 yielded the expected product size of 41 bp in purified γHV68 virions following infection of 3T12 cells, 3T12 cell debris after γHV68 infection, purified TKO.γHV68 virions following LE cell infection, and LE stably transfected cells. This confirms the packaging of miR-M1-10 in γHV68 virions, as well as the ability of TKO.γHV68 to package miR-M1-10 in trans.

RLM-RT-PCR analysis of miR-M1-12 yielded the expected product size of 43 bp in 3T12 cell debris after γHV68 infection and LE stably transfected cells. These products were not observed in either γHV68 virions following infection of 3T12 cells or TKO.γHV68 virions following LE cell infection, but identical doublets above the expected product size were observed. The doublets appear to be around 87 bp and 146 bp, potentially corresponding to the TMER 5 pre-miRNA stem loop 1 and stem loop 1 + stem loop 2. The products must be sequenced to confirm this hypothesis. It is also possible that faint bands in the 3T12 cell debris after TKO.γHV68 infection and mock uninfected 3T12 cells are of the same size, indicating the unknown products are non-specific and cellular.

Despite the identities of the unknown products, the presence of miR-M1-12 in both of the infected cell controls, but not the purified virions, demonstrates that miR-M1-12 may not be packaged by either γHV68 or TKO.γHV68. Combined with the proof of packaging of miR-M1-1, miR-M1-7-3p, and miR-M1-10, this potentially indicates packaging of viral miRNAs in γHV68 is selective. The results also attest to the lack of contamination in the purified virions, because miRNAs present in the infected cells were not identified in purified virion RNA.

γHV68Δ9473 packages biologically active miR-M1-1 and miR-M1-7-3p in trans. MiRNAs produced by γHV68 during lytic infection are known to be biologically functional (Diebel et al., 2010). We wanted to see if this functionality was shared by packaged miRNAs. The biological functionality of packaged viral miRNAs was assessed using the γHV68Δ9473 mutant virus. γHV68Δ9473 lacks the

entire left end of the γHV68 genome, and therefore cannot produce any of the TMERs or M1 through M4 (Clambey et al., 2002).

293 cells were transfected with a plasmid containing the left end of the γHV68 genome ("pLE-WT") and subsequently infected with γHV68Δ9473. The virus could therefore package viral miRNAs made from the pLE-WT plasmid in the transfected 293 cells. As a control, the same procedure was used on cells transfected with a TKO-plasmid. The TKO-plasmid does not produce TMERs, because it contains the left end of the γHV68 genome without the RNA pol III promoter elements of the TMER genes ("pLE-TKO"). Supernatants were collected for analysis post-infection (Figure 13A).

Dual luciferase assays were performed to measure potential biological activity of miR-M1-1 and miR-M1-7-3p packaged in the virion. All 293 cells were transfected with the pGL3-Control or pGL3-target firefly luciferase reporter plasmid, with targets for either miR-M1-1 or miR-M1-7-3p (Figure 13B, C). MiRNA associated with Ago-2 will cleave these complementary RNA sequences, diminishing the firefly expression in the cell (Figure 13C). The pRL-TK renilla luciferase plasmid was also transfected into all cells to serve as a transfection control. Cells serving as experimental controls were also transfected with the pLE-WT or pLE-TKO plasmids, to demonstrate the maximum potential of the biological activity of TMERs made in the firefly transfected cells. Supernatants from the various γHV68Δ9473 infections were added to the remaining experimental cells (Figure 13B).

Supernatants from the γHV68Δ9473 infections of pLE-WT transfected cells produced a 25% reduction in firefly signal compared to supernatants collected from the γHV68Δ9473 infections of pLE-TKO transfected 293 cells for miR-M1-1, and a 15% reduction for miR-M1-7-3p, with P values of .016 and .019, respectively (Figure 13D, E). This data demonstrates that γHV68Δ9473 also packages these miRNAs in trans, and that the packaged miRNAs are biologically functional upon infection.

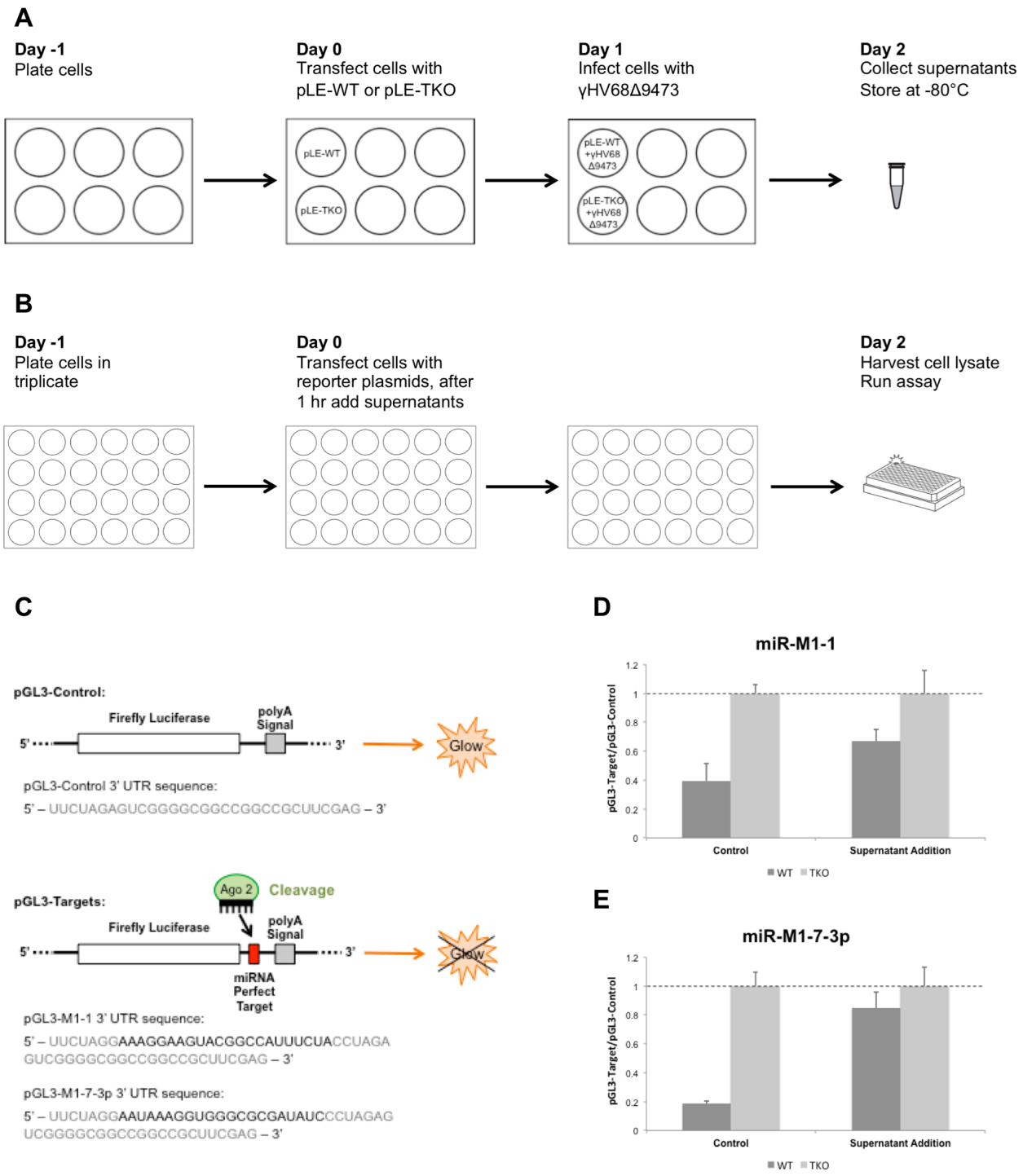

Figure 13. γHV68Δ9473 packages biologically active miR-M1-1 and miR-M1-7-3p in trans. (A) Schematic of initial transfections and supernatant collection. (B) Schematic of dual luciferase assay transfections and supernatant additions. (C) Schematic of pGL3-luciferase reporter plasmids. The pGL3-Control contains a short 3' UTR, while the pGL3-targets contain perfect complement sequences to miR-M1-1 and miR-M1-7-3p. Cleavage of these targets by miRNA Ago 2 complexes results in diminished firefly expression. (D/E) Dual luciferase reporter analysis from miR-M1-1 and miR-M1-7-3p. "Control" cells were transfected with pLE-WT (dark gray) and pLE-TKO (light grey). "Supernatant Addition" cells were exposed to supernatant from γHV68Δ9473 infection of pLE-WT transfected cells (dark gray) and pLE-TKO transfected cells (light gray).

Discussion

The field is only beginning to understand the roles of viral miRNAs in pathogenesis. MiRNAs potentially impact proliferation, immune recognition, viral lifecycles, and other biological processes during infection. Recent observations of biologically active packaged miRNAs have expanded our view of their potential roles in infection. Analysis of their targets could provide a novel window into numerous viral processes, such as latency and immune system evasion. The packaging of biologically active miR-M1-1 and miR-M1-7-3p, along with the previously identified tRNA-like portions of TMERs, make γHV68 a relevant model with which to study miRNA packaging.

This project has left us with many new directions to follow. We would first like to further explore the forms of packaged miRNAs. While we have confirmed the presence of maturely processed miR-M1-1 and miR-M1-7-3p with RLM-RT-PCR and sequencing, the RLM-RT-PCR procedure restricts us from identifying transcripts without 5' monophosphates. Northern blots, which allow us to see the full-length and pre-miRNA transcripts, are therefore a very useful tool. The unusual doublets we observed on the northern blots must be analyzed by running the samples along with RNA used in previous analyses where only three bands were identified. The lack of doublets in the RLM-RT-PCRs implies that the northern doublets are not a result of a modification that creates a 5' monophosphate, yet there is clearly some sort of degradation or modification process. Running samples together for the northern blot will provide us with a more exact comparison of transcript length.

A curious discrepancy between the northern blot and RLM-RT-PCR analyses is the lack of perfect pre-miR-M1-1 stem-loop 1 transcript in the sequenced RLM-RT-PCR product, when the northern blots clearly show its presence in the virion. We believe that this transcript has a 5' monophosphate and should be readily detectable by RLM-RT-PCR. The sequencing reactions demonstrated that the primers were not as specific as intended, so we will re-attempt the RLM-RT-PCR with higher annealing temperatures to yield more viral-specific products. This issue can also be avoided in future attempts to identify pre-miR-M1-1 stem-loop 1 by using inverse PCR. If we remain unable to amplify the perfect

pre-miR-M1-1 stem-loop 1, this potentially indicates that pre-miR-M1-1 stem-loop 1 lacks a 5' monophosphate, and the longer products we observed were degraded full-length transcript.

We would also like to explore the selectivity of miRNA packaging in γHV68. The products of the miR-M1-12 RLM-RT-PCR must first be cloned and sequenced to ensure its absence in the virion. The products we observed indicate that the precursors of miR-M1-12 are packaged in γHV68 as well as in trans by TKO.γHV68, but mature miR-M1-12 is not packaged. It will be interesting to see if this occurs with any other TMER miRNAs. We will expand the project to look at packaging of all of the TMERs encoded by γHV68, as well as their relative abundance.

In addition to the above directions, there are a few specific improvements this project will need before publication. We plan to add northern blots with the purified TKO.γHV68 virions and the controls used in RLM-RT-PCR. We will also add a control, purified TKO.γHV68 virions after infection of untransfected 3T12 cells. The dual luciferase assays must be rerun using TKO.γHV68, as the lab is currently transitioning from γHV68Δ9473 to TKO.γHV68 as the "TMER-less" viral control. The final step is proof of virion purification. Our strongest evidence involves the miR-M1-12 RLM-RT-PCR and other similar experiments, in which we saw evidence of miRNAs present in cell debris that were not present in purified virions. A series of detergent rinses and RNase treatments, as well as electron microscopy, are underway to provide conclusive evidence.

Future Projects

MiRNA targets

The most obvious next step for this project is to address the roles of packaged γHV68 miRNAs. Finding their specific targets may be difficult, as miRNAs require minimal complementarity for binding in mammalian cells. MiRNA targets do share characteristics, such as location in 3' UTRs, sequences of limited complementarity, and conservation across species. Viral miRNAs, however, do not share sequence conservation across species, so standard target scanning software is not effective (Diebel, 2009).

We will therefore rely on the narrow cell tropism of the virus to compare the seed sequences of viral and cellular miRNAs. Algorithm development and RNA arrays may also be used in the future.

RIG-I activation

Perhaps the most exciting part of this project involves another potential role of TMER miRNAs in the viral lifecycle. The van Dyk lab has recently been interested in the RIG-I–MAVS signaling pathway. This pathway results in triggering the type I interferon response in the cell; however, it also appears to play a role in transcriptional regulation for γHV68.

RIG-I (retinoic acid inducible gene I) is activated by 5' triphosphate RNA often transcribed by RNA pol III (Chiu et al., 2009). RIG-I then activates MAVS (mitochondrial antiviral signaling protein), and a signaling cascade ultimately results in the activation of NF-κB and the type I interferon response (Figure 14). Interestingly, MAVs also increases the transcription rate of γHV68 gene 50, which assists in the switch from early to late lytic infection. γHV68 therefore appears to take advantage of this pathway by entering the late stages of infection as soon as the immune response is triggered.

The van Dyk lab has previously observed viral miRNAs with 5' triphosphates during lytic infection. Our observations of doublets on northern blots undetectable using RLM-RT-PCR indicates the presence of miRNAs or miRNA precursors without 5' monophosphates in the virion. We would like to see if these packaged viral RNAs have 5' triphosphates, and if they play a role in activation of the RIG-I–MAVS pathway. Packaged miRNAs with 5' triphosphates would have the potential to activate this pathway immediately upon infection.

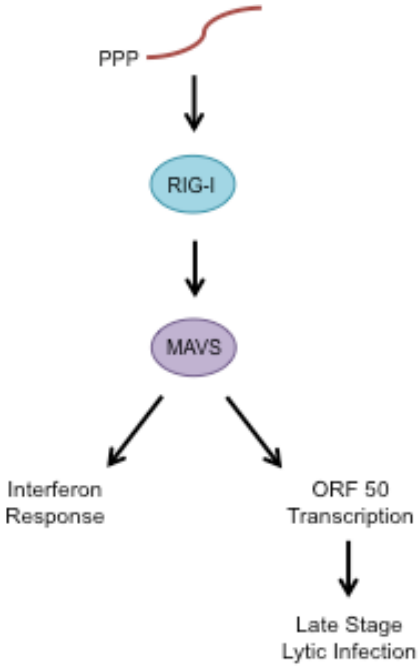

Figure 14. The RIG-I – MAVS signaling pathway. A very simplified schematic of the RIG-I – MAVS signaling pathway. 5' triphosphate RNA activates RIG-I, which activates MAVS. MAVS then triggers a signaling cascade resulting in the type I interferon response. MAVS also increases the transcription rate of γHV68 gene 50 (ORF 50), leading to late stage lytic infection.

Working on this project has been very exciting. We were able to accomplish our initial goals by finding proof of packaging and biological functionality of γHV68 miRNAs. Of course, we also opened the door to many new questions involving the packaging of TMER transcripts. I look forward to making the necessary adjustments to this project before publication, as well as the future projects to which this project leads.

Materials and Methods

Cell culture and viruses

The mouse fibroblast cell line 3T12 and human 293 epithelial cell line were cultured in Dulbecco's modified eagle media (DMEM) supplemented with 5% FBS (Hyclone), 2mM L-glutamine, 10 U/mL penicillin, and 10 μg/mL streptomycin sulfate. γHV68 (wild-type), TKO.γHV68 (TMER total knock-out), and γHV68Δ9473 (no left end) were used for all infections (Clambey et al., 2002; Diebel et al., in press). Virus stocks used had been passaged, grown, and titer determined as previously described (Virgin et al., 1997). In vitro infections for virion purifications were performed at a multiplicity of infection (MOI) of .05 plaque-forming units (PFU) per cell. In vitro infections for cellular debris analyses were performed at an MOI of 5 PFU per cell. In vitro infections in preparation for dual luciferase assays were performed at an MOI of 1 PFU per cell.

Virion purification

Virion purifications were performed as previously described (Cliffe et al., 2009). Six flasks of approximately 3.5 x 10^7 3T12 cells each were infected at an MOI of .05 PFU per cell. After 7 days, (complete cytopathic effect), the cell suspensions were centrifuged at 2,000*g* for 20 minutes at 4°C ("spin 1"). The resulting cellular debris pellets were stored at -80°C for future analysis. The supernatants were then combined and centrifuged at 20,000*g* for 2 hours at 4°C ("spin 2") to create a viral pellet. The viral pellet was resuspended in 15 mL DMEM (no supplements) and layered onto three 20% sucrose cushions (the contents of two cell flasks per sucrose cushion, effectively). These suspensions were ultra-centrifuged at 141,240*g* for 1 hour and 20 minutes at 4°C ("spin 3"). The resulting virion pellets were stored at -80°C for RNA isolation or future analysis.

RNA isolation

Isolations of total RNA (<200 nt) were performed using the *mir*Vana miRNA Isolation kit (Ambion), according to manufacturer's instructions.

Reverse ligation mediated RT-PCR

2 μg of total isolated RNA were combined with 10 ng of the RNA Linker Oligo or the 5'P-RNA Linker Oligo (Supplemental Table). This mixture was combined with 40 U of RNasin (Promega), 10 U of T4 RNA Ligase (New England BioLabs), and 5 μL of 10× T4 RNA Ligase reaction buffer. DEPC-treated RNase-free water was added to bring the reaction to 50 μL total volume, and the mixture was incubated for 30 min at 37°C. Following ligation, the reaction was heat inactivated at 65°C for 15 minutes. RNA was precipitated using 5 μL of NaOAc (pH 5.2) and 125 μL of 100% ethanol. The mixture was incubated at -80°C for a minimum of 20 min and pelleted at 13,200*g* for 15 min at 4°C. The pellet was washed with 200 μL of 70% ethanol, air dried for 5 min, and resuspended in 20 μL of DEPC-treated RNase-free water. 200 ng of ligated RNA were used as the template for RT-PCR amplification. The following RT-PCR cycling conditions were used: 50°C for 30 min, 95°C for 15 min, 40 amplification cycles of (94°C for 30 sec, 48°C for 30 sec, 72°C for 30 sec), and 72°C for 5 min. 25 μL of the reactions were run on 3% TAE agarose gels and products were visualized with ethidium bromide. For sequence confirmation of products, DNA was extracted from the gel using the QIAquick Gel Extraction Kit (Qiagen), and cloned using the TOPO TA Cloning Kit for Sequencing (Invitrogen).

Supplemental Table: Oligonucleotides for RLM-RT-PCR

Oligo	Sequence - 5' to 3'	Tm °C
RNA Linker Oligo	CUA CGA CAG UCA CCA CCG AUA CCC UGU ACU ACG CAC CAC G	N/A
5'P-RNA Linker Oligo	/5'P/CUA CGA CAG UCA CCA CCG AUA CCC UGU ACU ACG CAC CAC G	N/A
RNA Linker Outer Forward	CTA CGA CAG TCA CCA CCG ATA C	56.8
RNA Linker Inner Forward	CCC TGT ACT ACG CAC C	49.0
miR-M1-1 RLM-RT-PCR	GGA AGT ACG GCC ATT TC	50.5
pre-M1-1 RLM-RT-PCR	CTA TAG GGA TAA AGT TGG ACC C	53.0
miR-M1-7-3p RLM-RT-PCR	TAA AGG TGG GCG CGA TA	53.6
miR-M1-10 RLM-RT-PCR	AAA AGA ACC TTC CGT GTA A	48.0
miR-M1-12 RLM-RT-PCR	AAG GGG TAG GAC TCC CAC	49.0
mmu-miR-21 RLM-RT-PCR	AGC TTA TCA GAC TGA TGT TGA CTA	53.3

Small RNA Northern blot analysis

The miRNA marker ladder (New England BioLabs) and samples of 6 µg RNA were brought to final total volumes of 40 µL with gel loading buffer II (Ambion) and incubated for 5 min at 95°C. Samples were loaded into a 12% denaturing acrylamide gel with 7 M urea that had been prerun for 45 min at 65°C. The gel was then run for 70 min at 30 mA, stained with 1 µg/mL of ethidium bromide in 1× TBE for 5 min, and destained in 1× TBE for 2 min. The gel was transferred onto Zeta-Probe GT Genomic Tested Blotting Membrane (Bio-Rad) by semi-dry transfer at 500 mA for 1 hr in 1× TBE transfer buffer. An ultraviolet Stratalinker 1800 (Stratagene) was used to ultraviolet crosslink the membrane at 1200 × 100 µJ. 12 mL of formamide hybridization buffer (KPL) were mixed with 1200µg sheared and denatured herring sperm DNA, and incubated with the membrane for 1 hr at 54°C for prehybridization. 12 µL of 500 ng/ µL 59-biotinylated miR-M1-1 RNA probe or miR-M1-7-3p RNA probe were then denatured at 68°C for 10 min, and added to the hybridization mixture. The membrane was hybridized with the probe overnight at 54°C. After hybridization, the membrane was washed twice with 2× SSPE/0.5% SDS for 15 min at room temperature, washed twice with 2× SSPE/0.5% SDS for 30 min at 47°C, and washed once with 1× SSPE for 5 min at room temperature. Probes were detected with the KPL blotting kit (no. 54-30-02) according to the manufacturer's protocol. A 1:7000 dilution of AP-SA conjugate was used. The membrane was exposed using Blue Lite Autorad Film (ISC BioExpress) for 30 min, 90 min, and 18 hr.

Transfections

Transfections in preparation for dual luciferase assays, (for supernatant collection), were performed in duplicate in 6-well plates. Transfections for dual luciferase assays were performed in triplicate in 24-well plates. One day prior to transfection, 293 cells were trypsinized and resuspended in their standard growth media. 2 mL of 2×10^5 cell/mL were plated in 6-well plates and 500 µL of 1.6×10^5 cell/mL were plated in 24-well plates. Transfections were performed using Lipofectamine 2000 (Invitrogen) according to manufacturer's instructions. 6-well plates were transfected with 4000 ng of pLE-WT or 4000 ng of pLE-TKO per well. 24-well plates were transfected with 100 ng of pRL-TK and 50 ng of pGL3 (control or

target) alone, or combined with 440 ng of pLE-WT per well or 440 ng of pLE-TKO per well. Transfected cells were incubated until infection for supernatant collection or harvest for dual luciferase assays.

Supernatant collections

Cells were transfected in 6-well plates as described above, and infected after 24 hr with γHV68Δ9473 at an MOI of 1. Supernatants were collected after 24 hr in 250 μL aliquots and stored at -80°C before use in dual luciferase assays.

Dual luciferase assays

Dual luciferase assays were performed in triplicate in 24-well plates using the Dual-Luciferase Reporter Assay System (Promega) according to the manufacturer's instructions. In experiments involving the addition of viral supernatants, supernatants were added 1 hr post-transfection. 48 hr post-transfection, cells were washed with 250 μL of 1× PBS. 100 μL of 1× passive lysis buffer (PLB) was then added, and cells were rocked at room temperature for 15 min. Lysed cells were pipetted 20 times, and 20 μL of lysate were added to each well of a 96-well plate. The Bio-Tek Synergy HT microplate reader (BioTek) was used to collect luciferase readings. The reader dispensed 100 μL of Luciferase Assay Reagent II, took a 10 sec reading of the sample (Firefly luciferase value), dispensed 100 μL of Stop & Glo reagent, and took a 10 sec reading of the sample (Renilla luciferase value). The data were exported as an integral of the value of the reading taken. Photo multiplier tube sensitivity was set to 110.

Statistical analysis

Statistical analyses of the dual luciferase assay results were performed using Excel (Microsoft). Error values shown as error bars on bar graphs were calculated using the standard deviation function applied to normalized firefly luciferase values. P values were calculated using the Student's t-Test function using a paired, one-tailed distribution.

Acknowledgments

Above all, I would like to thank Linda van Dyk for providing me with the opportunity to learn and work at the University of Colorado School of Medicine. This project has been invaluable and life changing. I would also like to thank Kevin Diebel, for serving as my mentor on this project and spending countless hours providing input and advice. I look forward to working together to complete this project. Thanks also to Lauren Oko, for her advice and creation of the LE stably transfected cell line, and Maggie Medina, for her answers to my incessant questions. Finally, I would like to thank my thesis committee, Jennifer Martin, Nancy Guild, and Jennifer Kugel, for taking time to advise me on this project.

References

Amen, M., & Griffiths, A. (2011). Identification and Expression Analysis of Herpes B Virus-Encoded Small RNAs. *Journal of Virology*, *85*, 7296-7311.

Barton, E., Mandal, P., & Speck, S. (2011). Pathogenesis and Host Control of Gammaherpesviruses: Lessons from the Mouse. *Annual Review of Immunology*, *29*, 351-397.

Bowden, R., Simas, J., Davis, A., & Efstathiou, S. (1997). Murine gammaherpesvirus 68 encodes tRNA-like sequences which are expressed during latency. *Journal of General Virology*, *78*, 1675-1687.

Borchert, G., Lanier, W., & Davidson, B. (2006). RNA polymerase III transcribes human microRNAs. *Nature Structural & Molecular Biology*, *13*, 1097-1101.

Bortz, E., Whitelegge, J., Jia, Q., Zhou, Z., Stewart, J., Wu, T., et al. (2003). Identification of proteins associated with murine gammaherpesvirus 68 virions. *Journal of Virology*, *77*, 13425-13432.

Chiu, Y., Macmillan, J., & Chen, Z. (2009). RNA polymerase III detects cytosolic DNA and induces type I interferons through the RIG-I pathway. *Cell*, *138*, 576-591.

Clambey, E., Virgin, H., & Speck, S. (2002). Characterization of a spontaneous 9.5-kilobase-deletion mutant of murine gammaherpesvirus 68 reveals tissue-specific genetic requirements for latency. *Journal of Virology*, *76*, 6532-6544.

Cliffe, A., Nash, A., & Dutia, B. (2009). Selective Uptake of Small RNA Molecules in the Virion of Murine Gammaherpesvirus 68. *Journal of Virology*, *83*, 2321-2326.

Davison, A., Eberle, R., Ehlers, B., Hayward, G., McGeoch, D., Minson, A., et al. (2009). The order Herpesvirales. *Archives of Virology*, *154*, 171-177.

Diebel, K. (2009). *Biogenesis and biological functions of the gammaherpesvirus 68 encoded microRNAs*. (Unpublished doctoral dissertation). University of Colorado, Denver.

Diebel, K., & van Dyk, L. (in press). Gammaherpesvirus 68 total knockout virus.

Diebel, K., Smith, A., & van Dyk, L. (2010). Mature and functional viral miRNAs transcribed from novel RNA polymerase III promoters. *RNA*, *16*, 170-185.

He, L., & Hannon, G. (2004). MicroRNAs: Small RNAs with a Big Role in Gene Regulation. *Nature Reviews, 5*, 522-532.

Jochum, S., Ruiss, R., Moosmann, A., Hammerschmidt, W., & Zeidler, R. (2012). RNAs in Epstein-Barr virions control early steps of infection. *Proceedings of the National Academy of Sciences*, *109*, 1396-1404.

Lee, Y., Kim, M., Han, J., Yeom, K.-H., Lee, S., Baek, S., et al. (2004). MicroRNA genes are transcribed by RNA polymerase II. *The EMBO Journal*, *23*, 4051-4060.

Lin, X., Li, X., Liang, D., & Lan, K. (2012). MicroRNAs and Unusual Small RNAs Discovered in Kaposi's Sarcoma-Associated Herpesvirus Virions. *Journal of Virology*, *86*, 12717-12730.

Mettenleiter, T., Klupp, B., & Granzow, H. (2009). Herpesvirus assembly: an update. *Virus Research*, *143*, 222-234.

Peng, L., Ryazantsev, S., Sun, R., & Zhou, Z. (2010). Three-dimensional visualization of gammaherpesvirus lifecycle in host cells by electron tomography. *Structure*, *18*, 47-58.

Penkert, R., & Kalejta, R. (2011). Tegument protein control of latent herpesvirus establishment and animation. *Herpesviridae*, *2*.

Pfeffer, S., Sewer, A., Lagos-Quintana, M., Sheridan, R., Sander, C., Grässer, F., et al. (2005). Identification of microRNAs of the herpesvirus family. *Nature Methods*, *2*, 269-276.

Plaisance-Bonstaff, K., & Renne, R. (2011). Viral miRNAs. In R. van Rij, *Antiviral RNAi* (pp. 43-66). New York: Humana Press.

Schopman, N., van Montfort, T., Willemsen, M., Knoepfel, S., Pollakis, G., van Kampen, A., et al. (2012). Selective packaging of cellular miRNAs in HIV-1 particles. *Virus Research*, *169*, 438-447.

Reese, T., Xia, J., Johnson, L., Zhou, X., Zhang, W., & Virgin, H. (2010). Identification of Novel MicroRNA-Like Molecules Generated from Herpesvirus and Host tRNA Transcripts. *Journal of Virology*, *84*, 10344-10353.

Roizman, B., & Knipe, D. (2001). Herpes Simplex Viruses and Their Replication. In *Fields Virology* (pp. 2399-2459). Philadelphia: Lippincott Williams & Wilkins.

Roizman, B., & Pellet, P. (2006). The Family Herpesviridae: A Brief Introduction. In *Fields Virology* (pp. 2479-2499). Philadelphia: Lippincott Williams & Wilkins.

Thorley-Lawson, D. (2001). Epstein-Barr Virus: Exploiting the Immune System. *Nature Reviews Immunology*, *1*, 75-82.

Virgin, H., Latreille, P., Wamsley, P., Hallsworth, K., Weck, K., Dal Canto, A., et al. (1997). Complete sequence and genomic analysis of murine gammaherpesvirus 68. *Journal of Virology*, *71*, 5894-5904.

Virgin, H., & Speck, S. (1999). Unraveling immunity to gamma-herpesviruses: a new model for understanding the role of immunity in chronic virus infection. *Current Opinion in Immunology*, *11*, 371-379.

Zhu, J., Strehle, M., Frohn, A., Kremmer, E., Höfig, K., Meister, G., et al. (2010). Identification and Analysis of Expression of Novel MicroRNAs of Murine Gammaherpesvirus 68. *Journal of Virology*, *84*, 10266-10275.